Tumorigenesis in tuberous sclerosis complex is autophagy and p62/sequestosome 1 (SQSTM1)-dependent

Andrey Parkhitko[a,b], Faina Myachina[a], Tasha A. Morrison[a], Khadijah M. Hindi[a], Neil Auricchio[c], Magdalena Karbowniczek[d], J. Julia Wu[e], Toren Finkel[e], David J. Kwiatkowski[c], Jane J. Yu[a,1], and Elizabeth Petri Henske[a,1]

[a]Division of Pulmonary and Critical Care Medicine, Department of Medicine, Brigham and Women's Hospital and Harvard Medical School, Boston, MA 02115; [b]Department of Molecular Biology, Russian State Medical University, Moscow 117997, Russia; [c]Division of Translational Medicine, Department of Medicine, Brigham and Women's Hospital and Harvard Medical School, Boston, MA 02115; [d]School of Pharmacy, Texas Tech University Health Sciences Center, Abilene, TX 79601; and [e]National Heart Lung and Blood Institute, Bethesda, MD 20892

Edited by Eileen White, Cancer Institute of New Jersey, New Brunswick, NJ and accepted by the Editorial Board June 15, 2011 (received for review March 24, 2011)

Tuberous sclerosis complex (TSC) is a tumor suppressor syndrome characterized by benign tumors in multiple organs, including the brain and kidney. TSC-associated tumors exhibit hyperactivation of mammalian target of rapamycin complex 1 (mTORC1), a direct inhibitor of autophagy. Autophagy can either promote or inhibit tumorigenesis, depending on the cellular context. The role of autophagy in the pathogenesis and treatment of the multisystem manifestations of TSC is unknown. We found that the combination of mTORC1 and autophagy inhibition was more effective than either treatment alone in inhibiting the survival of tuberin (TSC2)-null cells, growth of TSC2-null xenograft tumors, and development of spontaneous renal tumors in *Tsc2*$^{+/-}$ mice. Down-regulation of Atg5 induced extensive central necrosis in TSC2-null xenograft tumors, and loss of one allele of *Beclin1* almost completely blocked macroscopic renal tumor formation in *Tsc2*$^{+/-}$ mice. Surprisingly, given the finding that lowering autophagy blocks TSC tumorigenesis, genetic down-regulation of p62/sequestosome 1 (SQSTM1), the autophagy substrate that accumulates in TSC tumors as a consequence of low autophagy levels, strongly inhibited the growth of TSC2-null xenograft tumors. These data demonstrate that autophagy is a critical component of TSC tumorigenesis, suggest that mTORC1 inhibitors may have autophagy-dependent prosurvival effects in TSC, and reveal two distinct therapeutic targets for TSC: autophagy and the autophagy target p62/SQSTM1.

metabolism | cell survival | therapy | chloroquine

Autophagy is increasingly recognized to play a critical role in tumor development and cancer therapy (1, 2). In autophagy, cells undergo membrane rearrangement to sequester a portion of cytoplasm, organelles, and intracellular proteins for delivery to a degradative lysosome for recycling. In situations of bioenergetic stress, autophagy promotes the survival of established tumors by supplying metabolic precursors; however, excessive autophagy has been associated with cell death (3, 4). Inhibition of autophagy using chloroquine (CQ), which blocks lysosome–autophagosome fusion and lysosomal protein degradation (5), suppresses the growth of Myc-induced lymphomas (6). In other situations, however, inhibition of autophagy promotes tumorigenesis; for example, haploinsufficinecy for the autophagy gene *Beclin1* promotes tumorigenesis in mouse models (7, 8), and allelic loss of *Beclin1* is associated with human breast, ovarian, and prostate cancers (1).

Tuberous sclerosis complex (TSC) is an autosomal dominant tumor suppressor gene syndrome caused by germline mutations in the *TSC1* or *TSC2* genes (9). Patients with TSC have multisystem manifestations, which can include neurologic disease (i.e., seizures, mental retardation, and autism), benign tumors in multiple organs, and pulmonary lymphangioleiomyomatosis (LAM). The TSC1-TSC2 protein complex acts as a cellular sensor, integrating signals from growth factors (10), hypoxia (11, 12), ATP availability (13), IκB kinase (IKK) (14), and the cell cycle (15) through direct phosphorylation by kinases that include AMPK, Akt, MAPK, IKKβ, and CDK1. The TSC2 protein contains an evolutionarily conserved GTPase-activating domain that regulates the small GTPase Rheb. Rheb directly activates the mammalian target of rapamycin complex 1 (mTORC1) (16). mTORC1 has at least two distinct sets of substrates: those that regulate protein translation via substrates that include p70S6K and 4EBP1 (17) and those that regulate autophagy. mTORC1 inhibits autophagy by direct phosphorylation of ULK1/2 kinases, thereby activating the ULK1/2/Atg13/FIP200 complex (18–20).

Little is known about the contribution of autophagy to tumorigenesis in TSC. Using genetic and pharmacologic approaches, we found that autophagy and the autophagy substrate p62/sequestosome 1 (SQSTM1) are critical components of TSC/mTORC1-driven tumorigenesis. These results have broad potential therapeutic implications for patients with TSC and other diseases resulting from dysregulation of the Akt/TSC/Rheb/mTORC1 signaling network.

Results

Survival of TSC2-Null Cells Is Dependent on Autophagy. To evaluate the role of tuberin in autophagy regulation, we compared basal autophagy in *Tsc2*$^{-/-}$*p53*$^{-/-}$ and *Tsc2*$^{+/+}$*p53*$^{-/-}$ murine embryonic fibroblasts (MEFs) (21). To monitor autophagy, we measured the conversion of LC3-I to LC3-II (22) and the level of p62/SQSTM1 protein that is degraded by autophagy (23). Tuberin-null MEFs had less LC3-II and more p62/SQSTM1 (Fig. 1*A*), along with fewer and smaller autophagosomes (Fig. 1*B*), indicating decreased autophagy levels. To monitor autophagic flux, cells were treated with the lysosomal inhibitor bafilomycin A, which led to accumulation of LC3-II in both *Tsc2*$^{+/+}$ and *Tsc2*$^{-/-}$ MEFs (Fig. S1 *A–C*). Densitometry analysis of LC3-II found a ratio of LC3-II treated/untreated with bafilomycin A

Author contributions: A.P., J.J.W., T.F., D.J.K., J.J.Y., and E.P.H. designed research; A.P., F.M., T.A.M., N.A., M.K., J.J.W., T.F., and J.J.Y. performed research; K.M.H. contributed new reagents/analytic tools; A.P., F.M., T.A.M., N.A., J.J.W., T.F., D.J.K., J.J.Y., and E.P.H. analyzed data; and A.P., J.J.Y., and E.P.H. wrote the paper.

The authors declare no conflict of interest.

This article is a PNAS Direct Submission. E.W. is a guest editor invited by the Editorial Board.

Freely available online through the PNAS open access option.

[1]To whom correspondence may be addressed. E-mail: jyu13@partners.org or ehenske@partners.org.

This article contains supporting information online at www.pnas.org/lookup/suppl/doi:10.1073/pnas.1104361108/-/DCSupplemental.

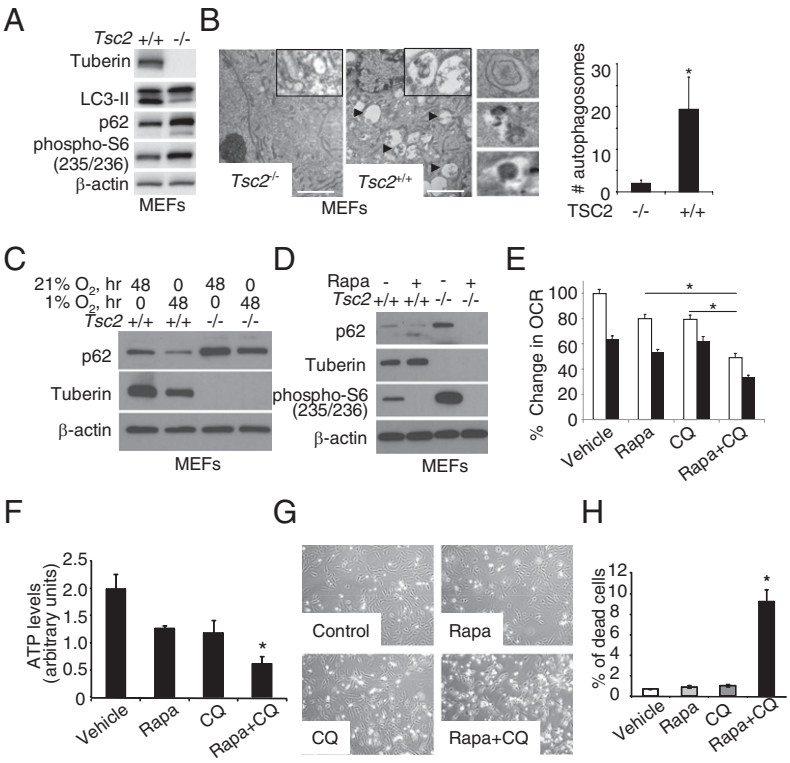

Fig. 1. Survival of TSC2-null cells is dependent on autophagy. (*A*) Immunoblot analysis of LC3-II and p62/SQSTM1 in $Tsc2^{+/+}$ and $Tsc2^{-/-}$ MEFs. (*B*) Transmission electron microscopy of $Tsc2^{+/+}$ and $Tsc2^{-/-}$ MEFs. (*Insets*) Representative autophagosomes and autolysosomes under higher magnification. (Scale bar: 2 μM.) The graph shows number of autophagosomes per cell. *$P < 0.05$. (*C*) Immunoblot analysis of p62/SQSTM1 and tuberin in $Tsc2^{+/+}$ and $Tsc2^{-/-}$ MEFs grown in normoxic (21% O_2) or hypoxic (1% O_2) conditions for 48 h. (*D*) Immunoblot analysis of p62/SQSTM1 in $Tsc2^{+/+}$ and $Tsc2^{-/-}$ MEFs treated with 20 nM rapamycin or vehicle for 24 h. (*E*) OCR measured using a Seahorse Bioscience XF24 analyzer after treatment of angiomyolipoma-derived TSC2-null 621-101 cells with CQ (10 μM), rapamycin (20 nM), or both for 24 h. Cellular respiration rate per million cells (OCR, pmol/min/million cells) is shown. Basal OCR (white bars) was measured for 20 min. Resting OCR (black bars) was measured in the presence of the ATP synthase inhibitor oligomycin (5 mM). Each data point represents mean ± SD; $n = 6$. *$P < 0.05$. (*F*) ATP levels measured using the PerkinElmer ATPlite assay system after treatment of ELT3 cells cultured in DMEM + 10% FBS with CQ (10 μM), rapamycin (20 nM), or both for 24 h. *$P < 0.05$. (*G*) Morphology of TSC2-null ELT3 cells cultured in serum-free, glutamine-free, and low-glucose (1 g/L) media after treatment with CQ (10 μM), rapamycin (20 nM), or both for 24 h. (*H*) Percentage of propidium iodide-positive ELT3 cells cultured and treated as described for 24 h. *$P < 0.05$.

of 5.4 in $Tsc2^{+/+}$ MEFs and 3.8 in $Tsc2^{-/-}$ MEFs (Fig. S1*B*), suggesting that autophagy flux may be lower in TSC2-null cells.

To evaluate the role of tuberin in autophagy regulation under stress conditions, we exposed $Tsc2^{-/-}p53^{-/-}$ and $Tsc2^{+/+}p53^{-/-}$ MEFs to hypoxic conditions (1% O_2) for 48 h. The level of hypoxia-induced autophagy, as measured by p62 accumulation, was lower in $Tsc2^{-/-}p53^{-/-}$ MEFs than in $Tsc2^{+/+}p53^{-/-}$ MEFs (Fig. 1*C*). To determine whether loss of tuberin results in p62 accumulation in vivo, we compared p62 levels in size-matched xenograft tumors from Tsc2-null ("V3") and TSC2-reexpressing ("T3") ELT3 cells (24). p62 levels were consistently higher in the Tsc2-deficient tumors (Fig. S2). To examine whether autophagy in tuberin-deficient cells is mTORC1-dependent, we treated $Tsc2^{-/-}p53^{-/-}$ and $Tsc2^{+/+}p53^{-/-}$ MEFs with 20 nM rapamycin for 48 h. mTORC1 inhibition decreased p62/SQSTM1 (Fig. 1*D*) and increased LC3-II in the presence of lysosomal inhibitors E64d and pepstatin (Fig. S3), indicating mTORC1-dependent autophagy regulation. Autophagy maintains energy homeostasis by providing substrate availability and recycles dysfunctional mitochondria. To determine whether autophagy is essential for mitochondrial respiration under regular growth conditions, we measured the oxygen consumption rate (OCR) in ELT3 cells treated with 20 nM rapamycin and/or 10 μg/mL of CQ for 24 h. CQ inhibits the fusion between lysosomes and autophagosomes, thereby blocking a late step of autophagy (25). The combination of rapamycin and CQ was more effective in reducing the OCR compared with either drug alone (Fig. 1*E*). In addition, the steady-state ATP level was lower with the combined treatment (Fig. 1*F*). We next measured the effects of rapamycin and CQ on the survival of ELT3 cells in nutrient-restricted DMEM [low glucose (1 g/L), serum- and L-glutamine free]. Neither drug alone induced cell death, but the combination of rapamycin and CQ for 24 h induced significant cell death (Fig. 1 *G* and *H*). Moreover, ELT3 cells were more sensitive to dual treatment than TSC2-reexpressing cells in normal (Fig. S4*A*) and nutrient-restricted conditions (Fig. S4*B*).

Dual Inhibition of Autophagy and mTORC1 More Effectively Suppresses TSC2-Null Tumor Development Than Inhibition of Either One Alone. To evaluate the role of autophagy in TSC2-null tumors in vivo, we treated mice bearing Tsc2-null ELT3 xenograft tumors with CQ. We found that CQ reduced tumor growth by ~40% compared with vehicle control (Fig. 2*A*, $P < 0.05$), suggesting that further decreases of autophagy in TSC2-null cells limits these cells' growth in vivo. As noted earlier, rapamycin induces autophagy in Tsc2-null cells (Fig. 1*D*), and the combination of rapamycin and CQ induces the death of Tsc2-null cells in vitro (Fig. 1 *G* and *H*). Thus, we next tested the combination of rapamycin and CQ on the growth of $Tsc2^{-/-}$ MEF xenograft tumors, which have a shorter tumor latency and more consistent growth kinetics than ELT3 cells. CQ treatment alone showed a trend toward reduced tumor growth ($P = 0.088$) (Fig. 2*B*). The combination of rapamycin and

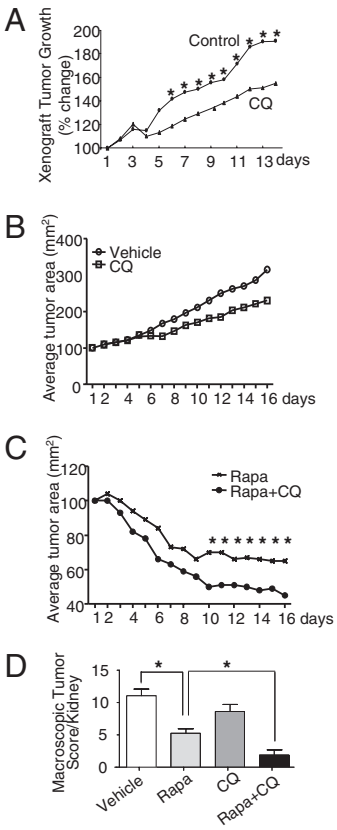

Fig. 2. Dual inhibition of autophagy and mTORC1 is more effective than inhibition of either agent alone in suppressing TSC2-null tumor development. (*A*) *SCID* mice bearing established TSC2-null ELT3 xenografts tumors were treated with vehicle control or CQ (50 mg/kg/d for 2 wk; $n = 12$ per group). *$P < 0.05$. (*B* and *C*) Nude mice bearing established $Tsc2^{-/-}$ MEF xenograft tumors were treated with vehicle control ($n = 4$), CQ (50 mg/kg/d) ($n = 4$) (*B*), rapamycin (6 mg/kg/d), or rapamycin (6 mg/kg/d) plus CQ (50 mg/kg/d) for 2 wk ($n = 8$ per group) (*C*). *$P < 0.05$. (*D*) $Tsc2^{+/-}$ mice in the A/J genetic background were treated with vehicle or with rapamycin (3 or 6 mg/kg, 3 times/wk), CQ (50 mg/kg/d), or both for 4–8 wk. Macroscopic kidney tumors were scored at age 5 mo. *$P < 0.05$.

CQ resulted in a greater reduction in tumor size compared with either drug alone ($P < 0.05$) (Fig. 2*C*). TUNEL staining revealed no differences in cell death (Fig. S5*A*).

To further analyze the in vivo effect of dual treatment with mTORC1 and autophagy inhibitors, we examined spontaneous renal tumorigenesis in $Tsc2^{+/-}$ mice in the A/J genetic background, which develop renal tumors at age 5 mo (26). Four mice receiving the combination of rapamycin (6 mg/kg i.p., 3 d/wk) and CQ (50 mg/kg i.p., 5 d/wk) required sacrifice after 1 wk because of delayed wound healing and/or infection at the site of ear tagging (which was performed on day 1 of treatment). Impaired wound healing is a well-known toxicity of rapamycin (27); therefore, the remaining mice received half the dose of rapamycin (3 mg/kg i.p., 3 d/wk) plus CQ during weeks 2–4. Despite this dose adjustment, the mice receiving the combined treatment had significantly fewer and smaller macroscopic lesions at age 5 mo than the mice receiving rapamycin alone at the higher dose (6 mg/kg i.p., 3 d/week for 4 wk) or CQ alone at the same dose (Fig. 2*D* and Fig. S6). TUNEL staining showed no differences in cell death (Fig. S5*B*).

Taken together, these in vivo data demonstrate that the combination of mTORC1 and autophagy inhibition is more effective than either treatment alone in suppressing both xenograft and spontaneous tumor growth.

ATG5 Is Required for TSC2-Null Xenograft Tumor Growth. To further investigate the impact of autophagy on TSC tumor growth, we down-regulated Atg5, an essential autophagy gene (28–30) in $Tsc2^{-/-}p53^{-/-}$ MEFs using GFP-Atg5 shRNAs. The level of Atg5 depletion as measured by qRT-PCR was 45% ($P < 0.01$), leading to a further increase of p62 (Fig. 3*A*). These cells were inoculated s.c. into nude mice. At 8 wk after cell inoculation, no differences in tumor size were seen, but tumor whole mounts showed extensive central necrosis in Atg5-shRNA tumors compared with control shRNAs (37% vs. 10%; $P < 0.05$) (Fig. 3*B*). Furthermore, immunoblot analysis revealed decreased GFP expression in GFP-Atg5-shRNA tumors (Fig. 3*C*), suggesting in vivo selection against cells with Atg5 knockdown. Moreover, Atg5 down-regulation in $Tsc2^{-/-}p53^{-/-}$ MEFs resulted in reduction of ATP levels in regular growth conditions (Fig. S7 *A–C*) and cell death in nutrient-restricted conditions (Fig. S7*D*).

Allelic Disruption of *Beclin1* Suppresses Spontaneous Renal Tumorigenesis in *Tsc2* Heterozygous Mice. We next examined the role of autophagy on spontaneous tumorigenesis in TSC. $Tsc2^{+/-}$ mice in the C57BL/6 background, which develop renal cystadenomas by age 9–10 mo (21), were crossed with $Beclin1^{+/-}$ mice (7, 8). *Beclin1* haploinsufficiency has been shown to suppress autophagy in vitro and in vivo (31, 32). Four mice per genotype were killed at 10 mo of age. Using a previously validated scoring system (33, 34), we found a striking difference in renal tumor incidence between $Tsc2^{+/-}$ and $Tsc2^{+/-}Beclin1^{+/-}$ mice (Fig. 4*A*). The average and median kidney lesion scores were 5.9 and 3.5, respectively, in the $Tsc2^{+/-}$ kidneys, vs. 1.3 and 0 in the $Tsc2^{+/-}Beclin1^{+/-}$ kidneys (Fig. 4*B*). No kidney lesions were observed in WT or $Beclin1^{+/-}$ kidneys. $Tsc2^{+/-}Beclin1^{+/-}$ kidneys also had significantly fewer microscopic kidney lesions compared with $Tsc2^{+/-}$ kidneys (Fig. 4 *C* and *D*). This indicates that disruption of one allele of *Beclin1* caused a major reduction in spontaneously arising renal tumors in $Tsc2^{+/-}$ mice. This result is particularly striking because *Beclin1* is a haploinsufficient tumor suppressor, further underscoring the context-dependent role of autophagy in tumorigenesis.

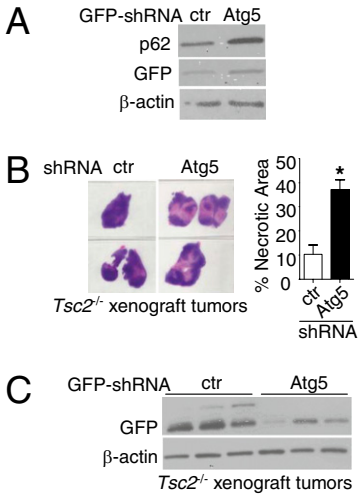

Fig. 3. ATG5 is required for TSC2-null xenograft tumor cell survival. (*A*) Immunoblot analysis of GFP and p62/SQSTM1 in $Tsc2^{-/-}$ MEFs infected with GFP-control or GFP-*Atg5* shRNA. (*B*) Whole-mount H&E staining of size-matched xenograft tumors of $Tsc2^{-/-}$ MEFs with GFP-control or GFP-*Atg5* shRNA. The percentage of necrotic area was determined by a blinded investigator using H&E-stained sections. *$P < 0.05$. (*C*) Immunoblot analysis of GFP in tumors from *B*.

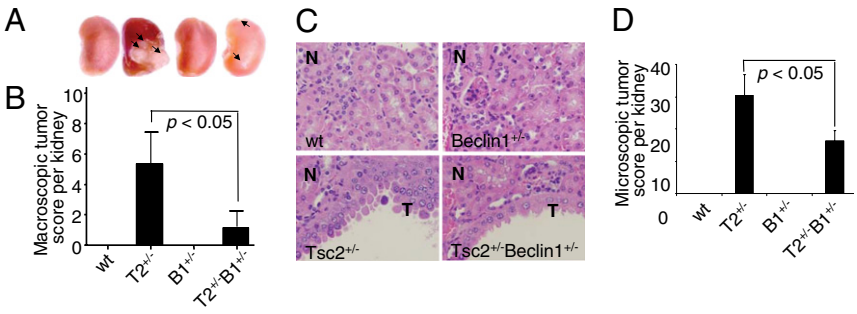

Fig. 4. Allelic disruption of *Beclin1* suppresses spontaneous renal tumorigenesis in *Tsc2* heterozygous mice. (*A*) The kidney with the most severe lesions from each genotype is shown; arrows indicate cystadenomas. (*B*) Macroscopic tumor scores from WT (wt), $Tsc2^{+/-}$ ($T2^{+/-}$), $Beclin1^{+/-}$ ($B1^{+/-}$), and $Tsc2^{+/-}Beclin1^{+/-}$ ($T2^{+/-}B1^{+/-}$) littermates (n = 8 kidneys per genotype). No tumors were observed in WT or $Beclin1^{+/-}$ mice. *$P < 0.05$. (*C*) Representative H&E-stained lesions. N, normal kidney. T, cystadenomas. (Original magnification, 20×.) (*D*) Microscopic tumor scores. *$P < 0.05$.

p62/SQSTM1 Is Required for TSC2-Null Tumor Development. We examined three human angiomyolipomas and found that all had strikingly higher levels of p62/SQSTM1 protein than normal kidney tissue from the same patient (Fig. 5*A*). Pulmonary LAM cells also expressed high levels of p62/SQSTM1 compared with adjacent cells (Fig. 5*B*).

p62/SQSTM1 promotes tumorigenesis (35, 36) via activation of the NF-κB and Nrf2 pathways. The high levels of p62/SQSTM1 in angiomyolipomas and LAM cells led us to hypothesize that p62/SQSTM1 promotes TSC tumorigenesis. To address this hypothesis, we down-regulated p62/SQSTM1 using shRNA in $Tsc2^{-/-}$ $p53^{-/-}$ MEFs. Although p62/SQSTM1 depletion did not affect LC3-II formation, cell survival, or proliferation in vitro (Fig. 5 *C* and *D*), decreased levels of phospho-p44/42 MAPK (Thr202/Tyr204) and phospho-IKKα/β (Ser176/180) phosphorylation were observed (Fig. 5*E*). $Tsc2^{-/-}$ MEFs with control or p62/SQSTM1 shRNA were inoculated s.c. bilaterally into SCID mice (n = 7 per group). p62/SQSTM1-shRNA delayed tumor growth by 6 wk ($P < 0.05$) (Fig. 5*F*). Only two of seven mice injected with p62/SQSTM1 shRNA cells developed single tumors, whereas five of seven mice injected with control shRNA cells developed bilateral tumors. Importantly, in the two tumors carrying the p62 shRNA, expression of p62/SQSTM1 was restored (Fig. 5*G*). These data indicate that p62/SQSTM1 is necessary for tumor formation by TSC2-null cells.

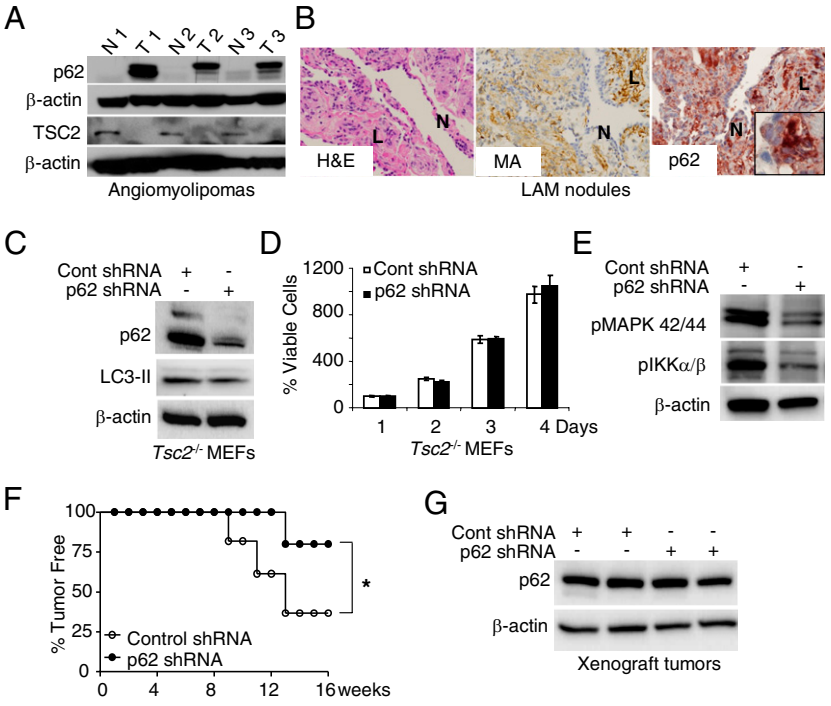

Fig. 5. p62/SQSTM1 is required for TSC2-null tumor development. (*A*) Immunoblot analysis of p62/SQSTM1 and tuberin (TSC2) in matched pairs of angiomyolipoma (T1–T3) and adjacent normal kidney (N1–N3). (*B*) Immunohistochemical analysis of p62/SQSTM1 accumulation in LAM nodules, which are positive for muscle actin. (Original magnification, 20× and 60×.) N, normal lung. L, LAM cells. (*C*) Immunoblot analysis of p62/SQSTM1 and LC3-II in $Tsc2^{-/-}$ MEFs stably infected with lentiviral control or p62/SQSTM1 shRNA. (*D*) Cell growth as assessed by the ATPlite cell viability assay. (*E*) Immunoblot analysis of phospho-p44/42 MAPK (Thr202/Try204) and phospho-IKKα/β (Ser176/180) in $Tsc2^{-/-}$ MEFs stably infected with lentiviral control or p62/SQSTM1 shRNA. (*F*) Kaplan–Meier plot of the percentage of tumor-free mice after inoculation with $Tsc2^{-/-}$ MEFs stably infected with lentiviral control or p62/SQSTM1 shRNA. *$P < 0.05$, Mantel–Cox log-rank test. (*G*) Immunoblot analysis of p62/SQSTM1 in xenograft tumors from *F*.

Discussion

In cancer (37, 38), autophagy can impact both tumor initiation and tumor progression, providing distinct opportunities for therapeutic targeting. Elucidating the contexts in which autophagy promotes tumor cell survival or induces tumor cell death is a critical step toward the optimization of autophagy-targeted agents. mTORC1 is a critical regulator of autophagy induction, via its direct phosphorylation of essential components of the autophagy machinery (39). TSC is a multisystem human disease in which tumors develop in the brain, skin, heart, lung, and kidney as a direct consequence of mTORC1 activation. Because of this tight link between the TSC-Rheb-mTORC1 signaling axis and autophagy, one might expect that the impact of autophagy on tumor formation and targeted therapy would be particularly striking in TSC. Therefore, we used in vitro and in vivo models of TSC to investigate the specific contribution of autophagy to mTORC1-driven tumorigenesis.

We found that autophagy is attenuated in TSC2-null cells under basal, nutrient-deprived, and hypoxic stress conditions. We hypothesized that because TSC2-null cells are unable to fully induce autophagy, TSC tumors might be highly dependent on autophagy during tumor progression. Consistent with this, treatment of mice bearing TSC2-null xenograft tumors with the Food and Drug Administration (FDA)-approved drug CQ inhibited tumor growth by ~40%, and cotreatment with rapamycin and CQ was more effective than either agent alone in suppressing xenograft tumors and spontaneous renal tumors. Down-regulation of Atg5, a component of the Atg12-Atg5-Atg16 complex, resulted in a threefold enhancement of necrosis in TSC2-null xenograft tumors. Most remarkably, disruption of one allele of *Beclin1* suppressed spontaneously arising macroscopic renal tumors in $Tsc2^{+/-}$ mice, strongly supporting the hypothesis that TSC tumors are autophagy-dependent. Our findings may be related to the recent observations that TSC2-null cells have multiple metabolic defects, including glutamine dependence (40) and abnormalities of glycolysis, the pentose phosphate pathway, and lipid biosynthesis (41), thereby increasing dependence on autophagy-generated metabolic precursors during tumor progression.

The results of the *Beclin1*/*Tsc2* cross are particularly revealing because *Beclin1* heterozygous mice develop lymphomas and tumors of the liver and lung (7, 8); yet, paradoxically, in the context of mTORC1 activation, *Beclin1* loss inhibited renal tumorigenesis. Defective autophagy has been observed in TSC1- and TSC2-null cells associated with defective aggresome formation (42) and response to reactive oxygen species (43), and inactivation of *TSC2* and *Rb* synergistically induces cell death via induction of oxidative stress (44). Despite these connections between TSC and oxidative stress, *Beclin1*/Tsc2 heterozygous mice exhibited a twofold decrease in microscopic lesions, indicating suppression of tumor initiation as well as tumor progression.

Low autophagy levels lead to accumulation of the autophagy substrate p62/SQSTM1, which promotes tumorigenesis via activation of NF-κB (35, 36) and Nrf2 (45). We found high levels of p62/SQSTM1 in angiomyolipomas and LAM cells. Depletion of p62/SQSTM1 dramatically delayed TSC2-null tumor development in a xenograft model. This finding is surprising given that genetic autophagy inhibition suppresses tumors in the TSC2-null xenografts and in the *Tsc2*/*Beclin1* mice; it may reflect a delicate balance between autophagy inhibition and autophagy activation in TSC tumorigenesis.

Our data demonstrate that inhibition of autophagy suppresses tumorigenesis in xenograft and endogenous models of TSC-mTORC1–driven tumors. Can these findings be used to optimize therapeutic strategies for patients with TSC and LAM? Treatment of patients with TSC and LAM with the mTORC1 inhibitor shrinks angiomyolipomas and subependymal giant cell astrocytomas, yet tumors regrow to approximately their original size when the agents are stopped (46–48). TORC1 inhibition potently induces autophagy in cells deficient in TSC1 or TSC2. Given our finding that TSC2-null tumors are highly autophagy-dependent, we speculate that rapamycin's partial clinical efficacy results from autophagy induction, inducing a nonproliferative "dormant" state. Therefore, autophagy inhibition may enhance the efficacy of mTORC1 inhibition in TSC and LAM. Importantly, CQ, used for malaria, and hydroxychloroquine (Plaquenil), used for rheumatoid arthritis, are FDA-approved agents. An important consideration is that the combination of CQ (50 mg/kg) and rapamycin (6 mg/kg) delayed wound healing at the site of ear-tagging in $Tsc2^{+/-}$ mice. This did not occur at the lower dose of rapamycin (3 mg/kg; Fig. 2*D*). Moreover, treatment of mice with xenograft tumors with CQ (50 mg/kg) and rapamycin (6 mg/kg) for 2 wk did not cause toxicity (Fig. 2*C*).

In conclusion, our data demonstrate that genetic and pharmacologic autophagy inhibition blocks tumorigenesis in xenograft and spontaneous models of TSC. Paradoxically, the autophagy substrate p62/SQSXM1, which accumulates in cells with low autophagy, is essential for tumor formation by TSC2-null cells. We hypothesize that the induction of autophagy by rapamycin provides a prosurvival stimulus, thereby contributing to the partial clinical response of human angiomyolipomas and subependymal giant cell astrocytomas to mTORC1 inhibition. We propose that dual inhibition mTORC1 and autophagy, using agents that are already FDA-approved, is a potential therapeutic strategy for TSC and LAM patients. Finally, we note that more than 100 clinical trials are currently underway using mTORC1 inhibitors. Because the TSC-Rheb complex is a direct regulator of mTORC1, genetic models of TSC can provide unique insights into the role of autophagy in the pathogenesis and treatment of human diseases associated with mTORC1 activation.

Methods

$Tsc2^{+/+}p53^{-/-}$ and $Tsc2^{-/-}p53^{-/-}$ MEFs (49), 621-101 cells (50), and ELT3 cells (24) were used. Autophagy was measured using LC3-I to LC3-II conversion, p62/SQSTM1 accumulation, and electron microscopy. Cell viability was measured by propidium iodide exclusion (40). Oxygen consumption was measured with a Seahorse Bioscience XF24 extracellular flux analyzer. Cellular ATP was measured with the ATPLite luminescence assay system (PerkinElmer). For xenograft tumor establishment, cells were inoculated bilaterally into the posterior back region of mice. Renal lesions in $Tsc2^{+/-}$ mice were scored using a standardized quantitative index (33, 34). Detailed descriptions of all methods are provided in *SI Methods*.

ACKNOWLEDGMENTS. We thank Beth Levine for providing the $Beclin1^{+/-}$ mice, Mustafa Sahin for providing the p62/SQSTM1 shRNA, Craig Thompson and Julian Lum for providing the Atg5 shRNA, and Michael Jarnik for performing TEM. This work was supported by the LAM Foundation, the Adler Foundation, the LAM Treatment Alliance, National Institute of Diabetes and Digestive and Kidney Diseases Grant DK51052 (to E.P.H.), National Heart, Lung, and Blood Institute Grant HL098216 (to J.J.Y.), and National Cancer Institute Grant P01 CA120964 (to D.J.K.). This research was conducted in partial fulfillment of A.P.'s doctoral degree requirements at the Department of Molecular Biology, Russian State Medical University, under the supervision of Dr. Olga Favorova.

1. Levine B, Kroemer G (2008) Autophagy in the pathogenesis of disease. *Cell* 132:27–42.
2. Mizushima N, Levine B, Cuervo AM, Klionsky DJ (2008) Autophagy fights disease through cellular self-digestion. *Nature* 451:1069–1075.
3. McPhee CK, Logan MA, Freeman MR, Baehrecke EH (2010) Activation of autophagy during cell death requires the engulfment receptor Draper. *Nature* 465:1093–1096.
4. Rabinowitz JD, White E (2010) Autophagy and metabolism. *Science* 330:1344–1348.
5. Solomon VR, Lee H (2009) Chloroquine and its analogs: A new promise of an old drug for effective and safe cancer therapies. *Eur J Pharmacol* 625: 220–233.
6. Amaravadi RK, et al. (2007) Autophagy inhibition enhances therapy-induced apoptosis in a Myc-induced model of lymphoma. *J Clin Invest* 117:326–336.
7. Qu X, et al. (2003) Promotion of tumorigenesis by heterozygous disruption of the beclin 1 autophagy gene. *J Clin Invest* 112:1809–1820.
8. Yue Z, Jin S, Yang C, Levine AJ, Heintz N (2003) *Beclin 1*, an autophagy gene essential for early embryonic development, is a haploinsufficient tumor suppressor. *Proc Natl Acad Sci USA* 100:15077–15082.
9. Crino PB, Nathanson KL, Henske EP (2006) The tuberous sclerosis complex. *N Engl J Med* 355:1345–1356.

10. Manning BD, Cantley LC (2007) AKT/PKB signaling: Navigating downstream. *Cell* 129: 1261–1274.
11. Brugarolas J, Kaelin WG, Jr. (2004) Dysregulation of HIF and VEGF is a unifying feature of the familial hamartoma syndromes. *Cancer Cell* 6:7–10.
12. Brugarolas J, et al. (2004) Regulation of mTOR function in response to hypoxia by REDD1 and the TSC1/TSC2 tumor suppressor complex. *Genes Dev* 18:2893–2904.
13. Inoki K, Zhu T, Guan KL (2003) TSC2 mediates cellular energy response to control cell growth and survival. *Cell* 115:577–590.
14. Lee DF, et al. (2007) IKK-β suppression of TSC1 links inflammation and tumor angiogenesis via the mTOR pathway. *Cell* 130:440–455.
15. Astrinidis A, Senapedis W, Coleman TR, Henske EP (2003) Cell cycle–regulated phosphorylation of hamartin, the product of the tuberous sclerosis complex 1 gene, by cyclin-dependent kinase 1/cyclin B. *J Biol Chem* 278:51372–51379.
16. Laplante M, Sabatini DM (2009) mTOR signaling at a glance. *J Cell Sci* 122:3589–3594.
17. Ma XM, Blenis J (2009) Molecular mechanisms of mTOR-mediated translational control. *Nat Rev Mol Cell Biol* 10:307–318.
18. Hosokawa N, et al. (2009) Nutrient-dependent mTORC1 association with the ULK1-Atg13-FIP200 complex required for autophagy. *Mol Biol Cell* 20:1981–1991.
19. Ganley IG, et al. (2009) ULK1.ATG13.FIP200 complex mediates mTOR signaling and is essential for autophagy. *J Biol Chem* 284:12297–12305.
20. Chang YY, Neufeld TP (2009) An Atg1/Atg13 complex with multiple roles in TOR-mediated autophagy regulation. *Mol Biol Cell* 20:2004–2014.
21. Onda H, Lueck A, Marks PW, Warren HB, Kwiatkowski DJ (1999) Tsc2(+/–) mice develop tumors in multiple sites that express gelsolin and are influenced by genetic background. *J Clin Invest* 104:687–695.
22. Kabeya Y, et al. (2000) LC3, a mammalian homologue of yeast Apg8p, is localized in autophagosome membranes after processing. *EMBO J* 19:5720–5728.
23. Bjørkøy G, et al. (2005) p62/SQSTM1 forms protein aggregates degraded by autophagy and has a protective effect on huntingtin-induced cell death. *J Cell Biol* 171: 603–614.
24. Howe SR, et al. (1995) Rodent model of reproductive tract leiomyomata: Establishment and characterization of tumor-derived cell lines. *Am J Pathol* 146:1568–1579.
25. Fedorko M (1967) Effect of chloroquine on morphology of cytoplasmic granules in maturing human leukocytes: An ultrastructural study. *J Clin Invest* 46:1932–1942.
26. Woodrum C, Nobil A, Dabora SL (2010) Comparison of three rapamycin dosing schedules in A/J $Tsc2^{+/-}$ mice and improved survival with angiogenesis inhibitor or asparaginase treatment in mice with subcutaneous tuberous sclerosis–related tumors. *J Transl Med* 8(14):1–18.
27. Buhaescu I, Izzedine H, Covic A (2006) Sirolimus—challenging current perspectives. *Ther Drug Monit* 28:577–584.
28. Kuma A, et al. (2004) The role of autophagy during the early neonatal starvation period. *Nature* 432:1032–1036.
29. Mizushima N, et al. (1998) A protein conjugation system essential for autophagy. *Nature* 395:395–398.
30. Mathew R, et al. (2007) Autophagy suppresses tumor progression by limiting chromosomal instability. *Genes Dev* 21:1367–1381.
31. Degenhardt K, et al. (2006) Autophagy promotes tumor cell survival and restricts necrosis, inflammation, and tumorigenesis. *Cancer Cell* 10:51–64.
32. Guo JY, et al. (2011) Activated Ras requires autophagy to maintain oxidative metabolism and tumorigenesis. *Genes Dev* 25:460–470.
33. Lee L, et al. (2005) Efficacy of a rapamycin analog (CCI-779) and IFN-γ in tuberous sclerosis mouse models. *Genes Chromosomes Cancer* 42:213–227.
34. Pollizzi K, Malinowska-Kolodziej I, Stumm M, Lane H, Kwiatkowski D (2009) Equivalent benefit of mTORC1 blockade and combined PI3K-mTOR blockade in a mouse model of tuberous sclerosis. *Mol Cancer* 8(38):1–9.
35. Duran A, et al. (2008) The signaling adaptor p62 is an important NF-κB mediator in tumorigenesis. *Cancer Cell* 13:343–354.
36. Mathew R, et al. (2009) Autophagy suppresses tumorigenesis through elimination of p62. *Cell* 137:1062–1075.
37. Kondo Y, Kanzawa T, Sawaya R, Kondo S (2005) The role of autophagy in cancer development and response to therapy. *Nat Rev Cancer* 5:726–734.
38. Mathew R, Karantza-Wadsworth V, White E (2007) Role of autophagy in cancer. *Nat Rev Cancer* 7:961–967.
39. Yu L, et al. (2010) Termination of autophagy and reformation of lysosomes regulated by mTOR. *Nature* 465:942–946.
40. Choo AY, et al. (2010) Glucose addiction of TSC null cells is caused by failed mTORC1-dependent balancing of metabolic demand with supply. *Mol Cell* 38:487–499.
41. Düvel K, et al. (2010) Activation of a metabolic gene regulatory network downstream of mTOR complex 1. *Mol Cell* 39:171–183.
42. Zhou X, et al. (2009) Rheb controls misfolded protein metabolism by inhibiting aggresome formation and autophagy. *Proc Natl Acad Sci USA* 106:8923–8928.
43. Alexander A, et al. (2010) ATM signals to TSC2 in the cytoplasm to regulate mTORC1 in response to ROS. *Proc Natl Acad Sci USA* 107:4153–4158.
44. Li B, Gordon GM, Du CH, Xu J, Du W (2010) Specific killing of Rb mutant cancer cells by inactivating TSC2. *Cancer Cell* 17:469–480.
45. Komatsu M, et al. (2010) The selective autophagy substrate p62 activates the stress responsive transcription factor Nrf2 through inactivation of Keap1. *Nat Cell Biol* 12: 213–223.
46. Bissler JJ, et al. (2008) Sirolimus for angiomyolipoma in tuberous sclerosis complex or lymphangioleiomyomatosis. *N Engl J Med* 358:140–151.
47. Franz DN, et al. (2006) Rapamycin causes regression of astrocytomas in tuberous sclerosis complex. *Ann Neurol* 59:490–498.
48. Krueger DA, et al. (2010) Everolimus for subependymal giant-cell astrocytomas in tuberous sclerosis. *N Engl J Med* 363:1801–1811.
49. Onda H, et al. (2002) Tsc2 null murine neuroepithelial cells are a model for human tuber giant cells, and show activation of an mTOR pathway. *Mol Cell Neurosci* 21: 561–574.
50. Yu J, Astrinidis A, Howard S, Henske EP (2004) Estradiol and tamoxifen stimulate LAM-associated angiomyolipoma cell growth and activate both genomic and non-genomic signaling pathways. *Am J Physiol Lung Cell Mol Physiol* 286:L694–L700.